Vol. 12, No. 2, 2021
ISSN 2233-4203/ e-ISSN 2093-8950
ARTICLE www.msletters.org | Mass Spectrometry Letters

Estimation of Phosphorus Concentration in Silicon Thin Film on Glass Using ToF-SIMS

M. Abul Hossion[1]*, Karthick Murukesan[2], and Brij M. Arora[3]

[1]*Department of Physics, Bangabandhu Sheikh Mujibur Rahman Maritime University, Dhaka 1216, Bangladesh*
[2]*Department of Electrical Engineering, University of Cambridge, Cambridge CB21PZ, United Kingdom*
[3]*Department of Physics, University of Mumbai, Mumbai 400098, India*

Received in May 26, 2021; Revised June 20, 2021; Accepted June 28, 2021
First published on the web June 30, 2021; DOI: 10.5478/MSL.2021.12.2.47

Abstract : Evaluating the impurity concentrations in semiconductor thin films using time of flight secondary ion mass spectrometry (ToF-SIMS) is an effective technique. The mass interference between isotopes and matrix element in data interpretation makes the process complex. In this study, we have investigated the doping concentration of phosphorus in, phosphorus doped silicon thin film on glass using ToF-SIMS in the dynamic mode of operation. To overcome the mass interference between phosphorus and silicon isotopes, the quantitative analysis of counts to concentration conversion was done following two routes, standard relative sensitivity factor (RSF) and SIMetric software estimation. Phosphorus doped silicon thin film of 180 nm was grown on glass substrate using hot wire chemical vapor deposition technique for possible applications in optoelectronic devices. Using ToF-SIMS, the phosphorus-31 isotopes were detected in the range of 10^1~10^4 counts. The silicon isotopes matrix element was measured from p-type silicon wafer from a separate measurement to avoid mass interference. For the both procedures, the phosphorus concentration versus depth profiles were plotted which agree with a percent difference of about 3% at 100 nm depth. The concentration of phosphorus in silicon was determined in the range of 10^{19}~10^{21} atoms/cm^3. The technique will be useful for estimating distributions of various dopants in the silicon thin film grown on glass using ToF-SIMS overcoming the mass interference between isotopes.

Keywords : ToF-SIMS, HWCVD, phosphorus, mass interference, RSF, thin film, glass

Introduction

An accurate quantification of the dopant profile in semiconductor is a complex task even today with the scaling down of devices such as, transistors[1] and thin film solar cell.[2] The dopants concentration in the semiconductor can be simulated using stopping and range of ions in matter (SRIM) computation code[3] from an ion implanted sample. For generalised samples, secondary ion mass spectrometry (SIMS) is widely used in the semiconductor material characterization.[4,5,6] The process allows the in-depth detection of various isotopes on the top or below the surface of a sample.[7] The mass interference between isotopes and matrix element makes the data interpretation process complex. Particularly, the detection of phosphorous in silicon suffers from the mass interference. The quantification of phosphorus or other dopant is critical for the performance of the electronics devices from various processes, such as, metal organic vapor phase epitaxy (MOVPE),[8] atomic layer deposition (ALD)[9] and chemical vapour deposition (CVD).[10] The analysis of phosphorus in the silicon thin films were executed in a high mass resolution ($m/\Delta m>10000$)[11] magnetic sector SIMS to separate phosphorus-31 (^{31}P) and hydrogenated silicon ($^{30}Si^1H$) isotopes.[12] The magnetic sector SIMS such as IMS-6f from Cameca, France, was used to eliminate the mass interference during data acquisition.[13,14] In the years 2010-2020, time of flight (ToF) SIMS is being widely used in academia due to its high sensitivity to trace elements, two dimensional elemental mapping (imaging) capacity, surface analysis of insulating/conducting material and the depth profiling at nano meter scale.[15] High depth resolution ToF-SIMS with charge compensation has also been used to examine secondary ion depth profiles relative to P and Si elements.[16]

In this article, phosphorus doped silicon thin film of 180 nm was grown on glass substrate using hot wire chemical vapor deposition (HWCVD) technique for possible applications in optoelectronic devices. The phosphorus

*Reprint requests to M. Abul Hossion,
https://orcid.org/0000-0002-3199-1682
E-mail: abulhossion.phy@bsmrmu.edu.bd

Table 1. Veeco Dektak 150 surface profiler data for the crater depth and the scanning length.

Sample name	Cursor position	Cursor width (mm)	X-axis position (mm)	Crater length (mm)	Y-axis position (nm)	Crater depth (nm)
Reference phosphorus	Left	0.08	0.1534	0.9028	0.9088	1137.18
	Middle	0.08	0.6049		-1093.40	
87-nSi-Glass	Right	0.08	0.9103	0.8764	0.6210	242.45
	Middle	0.08	0.4721		-243.31	

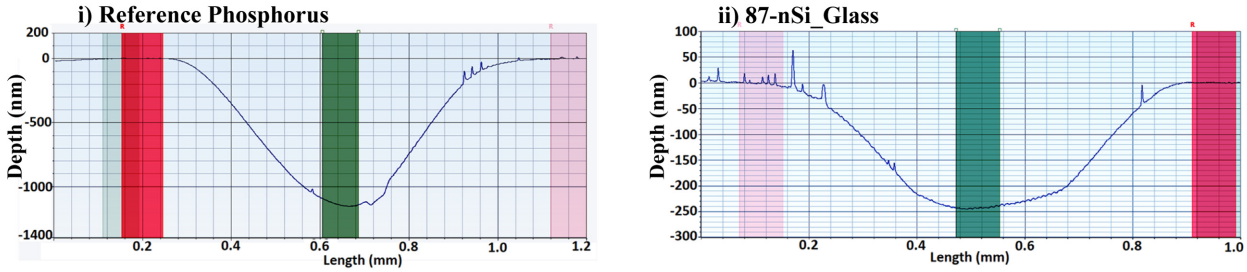

Figure 1. The total depth of the crater for i) reference phosphorus diffused silicon wafer is 1137.18 nm and for ii) 87-nSi-Glass phosphorus doped silicon thin film using HWCVD on glass is 242.45 nm measured using the Veeco Dektak 150 surface profiler.

concentration in the hydrogenated silicon thin film on glass was evaluated by ToF-SIMS using dynamic mode of operation. To avoid the mass interference, only ^{31}P isotope in silicon was measured. The matrix elements of silicon isotopes (^{30}Si, $^{30}Si^{1}H$) were detected in separate measurements. The quantitative analysis of counts to concentration conversion was done following two routes, standard relative sensitivity factor (RSF) with the silicon matrix element and SIMetric software (SW) estimation from reference sample without the silicon matrix element.

Experimental

Sample Preparation

Three samples were studied in this work. i) The phosphorus doped microcrystalline silicon thin films were grown on glass substrate using gas flow ratio of SiH_4:H_2:PH_3 = 2:50:1 sccm as an emitter layer in p-i-n diode[17]. The thin silicon film was synthesized by HWCVD technique at 350°C substrate temperature with a tantalum filament kept at a temperature of 1650°C.[18] The growth duration was 45 min for 180 nm thin film.[19] ii) An infrared laser from single emitter diode source with wavelength 1064 nm by SPI lasers limited, Germany was used to anneal the phosphorus doped silicon film on glass.[20] iii) The reference phosphorous sample was prepared in a diffusion furnace at 890°C for 15 min on 2 inch diameter n-type silicon wafer.[21] This diffusion process allows the phosphorus atoms to diffuse at about 600 nm.

Depth Profile analysis

The total crater depth was measured using the Veeco Dektak 150 surface profiler and the corresponding data is given in Figure 1 and Table 1. The sputtering rate for the Reference phosphorus diffused silicon wafer is 0.28 nm/s, where the crater depth is 1137.2 nm as shown in Figure 1(i) and total sputtering duration is 4020 s. The sputtering rate for 87-nSi-Glass phosphorus doped silicon thin film on glass using HWCVD is 0.30 nm/s, where the total crater depth is 242.5 nm as shown in Figure 1(ii) and total sputtering duration is 820 s.

ToF-SIMS data acquisition

To measure the secondary ion counts, the PHI nano ToF II TRIFT was used from Physical Electronics, MN, USA. In this process, a 10 ns pulsed liquid metal ion gun (LMIG) uses Gallium (Ga^+) sources to produce ions as primary ion beam to ionise the surface molecules.[22] The beam energy was kept 30 kV with a beam current of 15 nA and the raster size 300 × 300 μm^2.[23] The caesium ion (Cs^+) gun was used as sputtering tool to produce the negative secondary ions.[24] In the literature, dual beam IONTOF IV from Germany was used to profile phosphorus concentration with the Ga^+ ion gun at 25 kV, 1 pA for analysis and the Cs^+ ion gun at 1 kV, 80 nA for sputtering in the negative mode of operation.[25] In this study, the phosphorus isotope (^{31}P) was detected as secondary ions. The silicon isotope (^{30}Si) as the matrix elements were detected in a separate measurement from a p-type silicon wafer.[26] The ^{30}Si isotope counts was measured independently to avoid mass interference as well as to enhance the signal intensity.[27] The optimized scanning parameters for better depth resolution and improved detection limit are given in the Table 2.

Table 2. ToF-SIMS scanning parameters for the detection of phosphorus isotope (^{31}P) in silicon thin film using caesium ion (Cs^+) sputtering gun.

Sample Name	Phosphorus thin film thickness (nm)	Sputtering beam current (A)	Sputtering beam energy (kV)	Sputtering beam raster area (μm^2)	Sputtering duration (s)	Mass analyser analysing duration (s)
408-Reference phosphorus	1000					
421-87-nSi-Glass	180	8.23×10^{-8}	3	300 × 300	20	60
422-87-nSi-Glass-Laser	180					

Table 3. Part of the data for the conversion of ToF-SIMS counts to concentration-depth profile. The complete data set is provided as supportive material.

Crater depth [Cycle number × Sputtering Duration (s) × Sputtering rate (nm/s)] (nm)	Measured intensity of ^{31}P isotope (counts)	Measured intensity of ^{30}Si in p-type silicon wafer[26] (counts)	Phosphorus concentration (using Eq. 1) (atoms/cm^3)	Phosphorus concentration SIMetric SW estimation (using Eq. 2) (atoms/cm^3)	Percent difference (%)
i) 408-Reference phosphorus diffused silicon wafer					
5.66	3023	33616	3.07E+20	2.29E+20	29
11.32	2884	46138	2.13E+20	2.18E+20	2
16.97	2913	47072	*2.11E+20	**2.20E+20	4
ii) 421-87-nSi-Glass phosphorus doped silicon thin film on glass using HWCVD					
5.91	7947	33616	8.06E+20	6.01E+20	29
11.83	5800	46138	4.29E+20	4.38E+20	2
17.74	5192	47072	3.76E+20	3.93E+20	4
iii) 422-87-nSi-Glass-Laser phosphorus doped silicon thin film on glass using HWCVD					
5.91	10924	33616	1.11E+21	8.26E+20	29
11.83	15561	46138	1.15E+21	1.18E+21	2
17.74	15866	47072	1.15E+21	1.20E+21	4

*Using equation 1, $C_B = 1.1 \times 10^{23} \times 0.031 \times (\frac{2913}{47072}) = 2.11 \times 10^{20}$ atoms/cm^3

** Using equation 2, $C_B = 7.56 \times 10^{16} \times 2913 = 2.2 \times 10^{20}$ atoms/cm^3

Results and Discussion

The ToF-SIMS signal is interpreted using relative sensitivity factor for Phosphorus Counts to concentration conversion. The concentration of phosphorus (C_P) in silicon is calculated using the following equations; equation 1 using the silicon matrix element and equation 2 without the matrix element,[4]

$$C_P = RSF_{P(Si)} \times \%^{30}Si \times \left(\frac{I_{P(Si)}}{I_{30Si}}\right) \quad (1)$$

$$C_P = RSF_{P(Si).EST.} \times I_{P(Si)} \quad (2)$$

Here, C_P is Concentration of phosphorus in silicon, $RSF_{P(Si)}$ is the relative sensitivity factor of phosphorus in silicon,[28] $\%^{30}Si$ is the fractional isotope abundance of ^{30}Si isotope in silicon,[29] $I_{P(Si)}$ is the intensity of phosphorus isotope (^{31}P) counts using Cs^+ gun, I_{30Si} is the intensity of silicon isotope (^{30}Si) counts on a p-type silicon wafer[26] using ToF-SIMS and $RSF_{P(Si).EST.}$ is the relative sensitivity factor of phosphorus in silicon estimated using SIMetric SW peak fitting tool from the 408-Rreference phosphorus diffused silicon wafer. Table 3 shows the part of data used in the phosphorus counts to concentration conversion calculation. The complete data table is provided with the article as supplementary material.

The Table 3 is used to plot phosphorus concentration versus crater depth curve for the i) Reference Phosphorus, ii) 87-nSi-Glass and iii) 87-nSi-Glass-Laser as shown in Figure 2 and 3 respectively. Figure 2 shows the concentration of phosphorus, diffused in n-type silicon wafer for Reference Phosphorus sample along with the SIMetric SW estimated curve. The concentration of phosphorus at the top surface of the silicon wafer is 2×10^{20} atoms/cm^3, which is in agreement with the value 4.3×10^{20} atoms/cm^3 obtained using CAMECA SC Ultra high resolution SIMS by Beljakowa et al..[9] Figure 3 shows the concentration of phosphorus in (i) 180 nm microcrystalline silicon thin film grown on glass using HWCVD and (ii) infrared laser (1064 nm) annealed micro crystalline silicon thin film grown on glass using HWCVD along with the corresponding SIMetric SW estimated curve respectively. From Figure

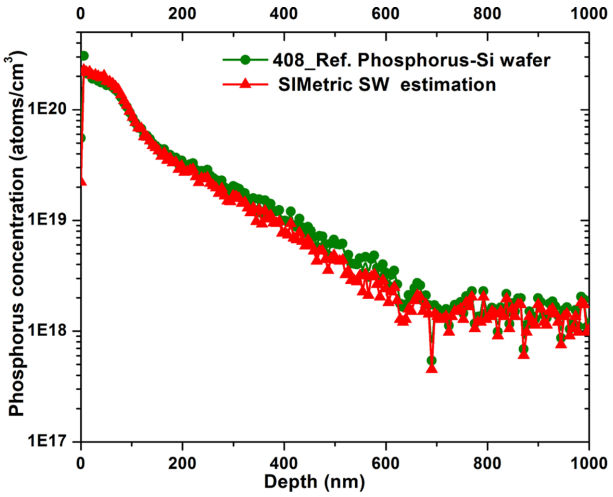

Figure 2. Phosphorus concentration – depth curve of sample 408_Ref.Phosphorus-Si wafer.

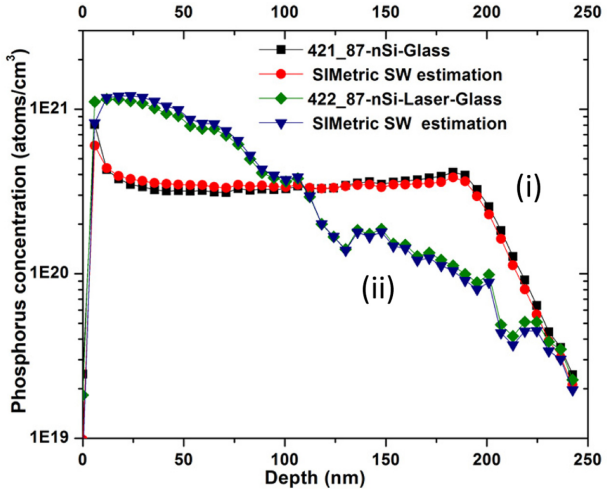

Figure 3. Phosphorus concentration – depth curve of sample (i) 421_87-nSi-Glass, and (ii) 422_87-nSi-Laser-Glass.

3(i), the concentration of phosphorus thin film is 3.25×10^{20} atoms/cm^3 at the top and this remain uniform over the top 180 nm. The Figure 3(ii) shows that, the laser irradiation caused significant changes in the thin film. It is seen that after the laser irradiation, the phosphorus concentration is no longer uniform. It has increased to 1.2×10^{21} atoms/cm^3 near the surface of the sample and decreased along the film thickness. This non-homogeneous laser absorption of silicon thin film is characterised using Raman imaging which is published elsewhere.[30] Furthermore, with laser irradiation, the silicon film melts and then starts to solidify from the position closest to the glass substrate. So, the film at the top surface solidifies later. The phosphorus has a segregation coefficient of around 0.35 which leads to an increase in the phosphorus concentration at the top surface as the top portion solidifies first.[31,32] The phosphorus concentration versus depth profiles of the RSF calculated and the SIMetric SW estimated are in agreement with a percent difference of about 3% at 100 nm depth, 12% at 200 nm, 20% 300 nm and 25% at 400 nm.

Conclusion

The concentration of phosphorus in silicon thin film grown on glass using HWCVD was estimated using ToF-SIMS technique in dynamic mode of operation. A phosphorus diffused silicon wafer was used as reference sample. The relative sensitivity factor along with silicon matrix element was used to interpret the ToF-SIMS data for each sample. Using SIMetric SW peak fitting tool, with the reference sample, the RSF was determined without the silicon matrix element data. The phosphorus counts to concentration conversion was performed using two routes, calculated RSF with silicon matrix element and simulated RSF procedure from reference sample. For the both procedures, the phosphorus concentration versus depth profiles were plotted which agree with a percent difference of about 3% at 100 nm depth. The concentration of phosphorus in silicon was determined in the range of 10^{19}~10^{21} atoms/cm^3 which is comparable with the value obtained using magnetic sector high resolution SIMS. The phosphorus in silicon detected on the top surface of phosphorus doped silicon thin film on glass was 3.25×10^{20} atoms/cm^3. The results of this study will be useful for the detection and quantification of impurities in wide area of thin films using ToF-SIMS technique overcoming the mass interferences between isotopes.

Acknowledgement

The authors thank, Jürgen Weippert, Fraunhofer Institute for Applied Solid State Physics, Freiburg, Germany, for the suggestions in data interpretation. The authors also thank, Dr. C. S. Harendranath, Principle research scientist, Sophisticated analytical instrument facility, Indian Institute of Technology Bombay, Mumbai, India, for providing ToF-SIMS laboratory facilities. The authors are grateful to Mr. Subhash Lokhre and Mr. Nilesh Marle for their active participation during the measurement process. We are grateful to HWCVD system team, Dr. Rajiv O. Dusane and Dr. Nilesh Wadibhasme, from the Department of Metallurgical Engineering and Materials Science, Indian Institute of Technology Bombay, Mumbai, India. We are also grateful to National Centre for Photovoltaic Research and Education (NCPRE) for allowing us to use the laser annealing tool.

Author Contributions

The authors Abul Hossion (A.H) and Brij Mohan Arora (B.M.A) participated in the conceptualization, designing

methodology, analysis, interpretation, discussion and improvement of the manuscript of the experimental data on ToF-SIMS study on phosphorus doped silicon film. Karthick Murukesan (K.M) prepared the reference sample and participated in the interpretation of SIMS data. A.H collected and analysed the data followed by the manuscript preparation while B.M.A does the review, editing, supervision and funding acquisition. All the figures and images are prepared by A.H. All the authors have read and agreed to this version of the manuscript.

Funding

This research was funded by Centre of Excellence in Nano electronics (CEN) of the Indian Institute of Technology, Bombay, Mumbai, India.

Conflicts of Interest

The authors declare no conflict of interest. The funders had no role in the design of the study; in the collection, analysis, or interpretation of data; in the writing of the manuscript, or in the decision to publish the results.

Supplementary Information

Supplementary information is available at https://drive.google.com/file/d/1TGFndqfANq9wCcfVK9HT3XT8J5fJF3ya/view?usp=sharing.

References

1. Yeoh, W. K.; Hung, S.-W.; Chen, S.-C.; Lin, Y.-H.; Lee, J. J. *Surf. Interface Anal*. **2020,** 52, 318, DOI: 10.1002/sia.6706.
2. Chen, H.-L.; Cattoni, A.; de Lépinau, R.; Walker, A. W.; Höhn, O.; Lackner, D.; Siefer, G.; Faustini, M.; Vandamme, N.; Goffard, J.; Behaghel, B.; Dupuis, C.; Bardou, N.; Dimroth, F.; Collin, S. *Nat. Energy* **2019,** 4, 761, DOI: 10.1038/s41560-019-0434-y.
3. Nipoti, R.; Parisini, A.; Boldrini, V.; Vantaggio, S.; Gorni, M.; Canino, M.; Pizzochero, G.; Camarda, M.; Woerle, J.; Grossner, U. *Mater. Sci. Forum* **2020,** 1004, 698, DOI: 10.4028/www.scientific.net/MSF.1004.698.
4. van der Heide, P. *Secondary Ion Mass Spectrometry: An Introduction to Principles and Practices*, *1st ed*. Wiley & Sons: New York, **2014**.
5. Riviere, J. C.; Myhra, S.; Myhra, S. *Handbook of Surface and Interface Analysis: Methods for Problem-Solving, 2nd Ed*. CRC Press: New York, **2009,** DOI: 10.1201/9781420007800.
6. Wilson, R. G. *Secondary Ion Mass Spectrometry: a Practical Handbook for Depth Profiling and Bulk Impurity Analysis*. Wiley & Sons: New York, **1989**.
7. Benninghoven, A.; Rudenauer, F. G.; Werner, H. W. *Secondary Ion Mass Spectrometry: Basic Concepts, Instrumental Aspects, Applications and Trends,* Wiley & Sons: New York, **1987**.
8. García-Tabarés, E.; Martín, D.; García, I.; Rey-Stolle, I. *Sol. Energy Mater. Sol. Cells* **2013,** 116, 61, DOI: 10.1016/j.solmat.2013.04.003.
9. Beljakowa, S.; Pichler, P.; Kalkofen, B.; Hübner, R. *Phys. Status Solidi A* **2019,** 216, 1900306. DOI: 10.1002/pssa.201900306.
10. Engelhardt, J.; Kromer, H.; Hahn, G.; Terheiden, B. AIP Conf. Proc. **2019,** 2147, 070002. DOI: 10.1063/1.5123863.
11. Maharrey, S.; Bastasz, R.; Behrens, R.; Highley, A.; Hoffer, S.; Kruppa, G.; Whaley, J. *Appl. Surf. Sci.* **2004,** 231–232, 972, DOI: 10.1016/j.apsusc.2004.03.197.
12. Li, Y.; Wang, S.; Lin, X.-F.; Wei, L. *Mater. Res. Soc. Symp. Proc.* **2005,** 862, 183, DOI: 10.1557/PROC-862-A18.3.
13. Loesing, R.; Guryanov, G. M.; Hunter, J. L.; Griffis, D. P. *J. Vac. Sci. Technol. B* **2000,** 18, 509, DOI: 10.1116/1.591222.
14. Hervig, R. L.; Mazdab, F. K.; Williams, P.; Guan, Y.; Huss, G. R.; Leshin, L. A. *Chem. Geol.* **2006,** 227, 83, DOI: 10.1016/j.chemgeo.2005.09.008.
15. Guilhaus, M. *J. Mass Spectrom.* **1995**, 30, 1519, DOI: 10.1002/jms.1190301102.
16. Mastromatteo, M.; Arduca, E.; Napolitani, E.; Nicotra, G.; Salvador, D. D.; Bacci, L.; Frascaroli, J.; Seguini, G.; Scuderi, M.; Impellizzeri, G.; Spinella, C.; Perego, M.; Carnera, A. *Surf. Interface Anal*. **2014,** 46, 393, DOI: 10.1002/sia.5578.
17. Hossion, A.; Khatavkar, S.; Arora, B. M. *J. Optoelectron. Adv. Mater.* **2021,** 23, 145.
18. Agarwal, M.; Pawar, A.; Wadibhasme, N.; Dusane, R. *Sol. Energy* **2017,** 144, 417, DOI: 10.1016/j.solener.2017.01.039.
19. Hossion, M. A.; Mondal, S.; Arora, B. M. *J. Russ. Laser Res.* **2020,** 41, 552, DOI: 10.1007/s10946-020-09910-9.
20. Mondal, S.; Solanki, C. S. *Mater. Sci. Semicond. Process*. **2017,** 59, 10, DOI: 10.1016/j.mssp.2016.11.011.
21. Murukesan, K.; Kumbhar, S.; Kapoor, A. K.; Dhaul, A.; Saravanan, S.; Pinto, R.; Arora, B. M. *$POCl_3$ Diffusion Process Optimization for the Formation of Emitters in the Crystalline Silicon Solar Cells; 2014 IEEE 40th Photovoltaic Specialist Conference (PVSC),* Denver (USA), 8-13 June 2014, p 3011, DOI: 10.1109/PVSC.2014.6925567.
22. Bayly, A. R.; Waugh, A. R.; Anderson, K. *Nucl. Instrum. Methods Phys. Res*. **1983**, 218, 375, DOI: 10.1016/0167-5087(83)91009-8.
23. Kia, A. M.; Haufe, N.; Esmaeili, S.; Mart, C.; Utriainen, M.; Puurunen, R. L.; Weinreich, W. *Nanomaterials* **2019,** 9, 1035, DOI: 10.3390/nano9071035.
24. Magee, C. W. *J. Electrochem. Soc*. **1979,** 126, 660, DOI: 10.1149/1.2129104.
25. Perego, M.; Caruso, F.; Seguini, G.; Arduca, E.; Mantovan, R.; Sparnacci, K.; Laus, M. *J. Mater. Chem. C*

2020, 8, 10229, DOI: 10.1039/D0TC01856B.
26. Hossion, M. A.; Arora, B. M. *Mass Spectrom. Lett.* **2021,** 12, 26, DOI: 10.5478/MSL.2021.12.1.26.
27. Stephan, T. *Planet. Space Sci.* **2001,** 49, 859, DOI: 10.1016/S0032-0633(01)00037-X.
28. Stevie, F. *Secondary Ion Mass Spectrometry: Applications for Depth Profiling and Surface Characterization*. Momentum Press: New York, **2015**.
29. Meija, J.; Coplen, T. B.; Berglund, M.; Brand, W. A.; Bièvre, P. D.; Gröning, M.; Holden, N. E.; Irrgeher, J.; Loss, R. D.; Walczyk, T.; Prohaska, T. *Pure Appl. Chem.* 2016, 88, 265, DOI: 10.1515/pac-2015-0305.
30. Hossion, A.; Maliakkal, C. B.; Mahmood, Z. H.; Arora, B. M. *Raman analysis of intrinsic and laser annealed n-type silicon film grown on glass using hot wire chemical vapor deposition; 2018 4th International Conference on Electrical Engineering and Information Communication Technology (ICEEiCT)*, Dhaka (Bangladesh) 13-15 September 2018, p 182, DOI:10.1109/CEEICT.2018.8628133.
31. Oberbeck, L.; Curson, N. J.; Hallam, T.; Simmons, M. Y.; Bilger, G.; Clark, R. G. *Appl. Phys. Lett.* **2004,** 85, 1359, DOI: 10.1063/1.1784881.
32. Nakano, S.; Liu, X.; Han, X.-F.; Kakimoto, K. *Crystals* **2021,** 11, 27, DOI: 10.3390/cryst11010027.

